# Humidity Sensing Properties of Nanoporous $TiO_2$-$SnO_2$ Ceramic Sensors

**Hye-Kyung Kim, Shivaram Dattatraya Sathaye, Young Kyu Hwang,* Sung Hwa Jhung, Jin-Soo Hwang, Soo Hwan Kwon,† Sang-Eon Park,‡ and Jong-San Chang***

*Research Center for Nanocatalysts, Korea Research Institute of Chemical Technology, P.O. Box 107, Yuseong, Daejeon 305-600, Korea. *E-mail: jschang@krict.re.kr*
*†Department of Chemistry and Korea Basic Science Institute, Chungbuk University, Cheongju 361-769, Korea*
*‡Department of Chemistry, Inha University, Incheon 402-751, Korea*
*Received August 9, 2005*

**Key Words :** Humidity sensor, $TiO_2$, $TiO_2$-$SnO_2$, Mesoporous, Ceramic sensor

Sensors have become an integral part of all the activity of modern human being. Amongst the sensors, humidity sensor is a vital requirement of human life and industrial applications and therefore needs exact monitoring. Although humidity sensors designed from ceramic materials, polymers and composites have been studied, ceramic sensors are preferred for their chemical and physical stability in an environment, which is suitable for its applications, processing ability and possibility of achieving predetermined properties.[1-5]

Although many oxides such as $SnO_2$,[1] ZnO,[2] $TiO_2$,[3] $ZrO_2$[4] $SiO_2$[5] are being studied for the development of humidity sensors, the research for newer methods and the materials is unending because of specific requirements of various applications in terms of sensitivity, selectivity, response time, low cost of manufacture, compactness and microprocessor compatibility. Moreover, it is almost impossible to develop an ideal universal humidity sensor for all applications.

$TiO_2$ based humidity sensors are studied vigorously, as it is likely to show better sensitivity because of its hydrophilic property.[3] It is studied more in thin film form.[6] However, it is reported that thin film sensors show lower sensitivity than those shown by porous ceramic sintered counterparts.[7-9] $TiO_2$ is known to have a hysteresis in humidity sensitivity curve. It was thought that the use of additives would be useful to get over this drawback. The additives are reported to minimize the hysteresis in $TiO_2$ humidity sensors.[10] Additives are also reported to improve performance parameters of $TiO_2$ humidity sensors.[11-15] $SnO_2$ is known as isostructural to a rutile phase of $TiO_2$ and fairly good electrical conductor was considered preferentially as an additive. $SnO_2$ has been independently studied and found to be a suitable sensor material for wide range of applications with its defect structure and variable oxidation state of Sn.

Since the mechanism of humidity sensors is mainly associated with adsorption desorption processes, the surface area of the sensors becomes an important factor to determine the sensing properties. The porosity can enhance the surface area and therefore the porous materials are considered as better sensor materials.[16] Although thin films have many advantageous properties for sensor applications, achieving porous thin films by use of energy intensive thin film formation processes has remained an unsolved problem for the scientists. It is known that porous $TiO_2$ can be synthesized by using polymer-dispersing agents which inspired us to attempt the development of porous $TiO_2$-based ceramic humidity sensors.

In the present work, the humidity sensing properties of $TiO_2$-$SnO_2$ ceramic pellets are investigated. The porosity of the pellets is monitored by the use of polymer dispersing agent in the processing of precursors and also maintaining low temperature for the formation of material. The humidity sensing properties are correlated to the various parameters namely, composition, structure, surface morphology of the material etc. Nanoporous $TiO_2$-$SnO_2$ sensor was prepared with block co-polymer, F127, as a dispersing agent as described in Scheme 1.

Figure 1 shows the XRD patterns for pure $TiO_2$, pure $SnO_2$ and $Ti_{1-x}Sn_xO_2$ film compositions where X = 0, 0.1, 0.3, and

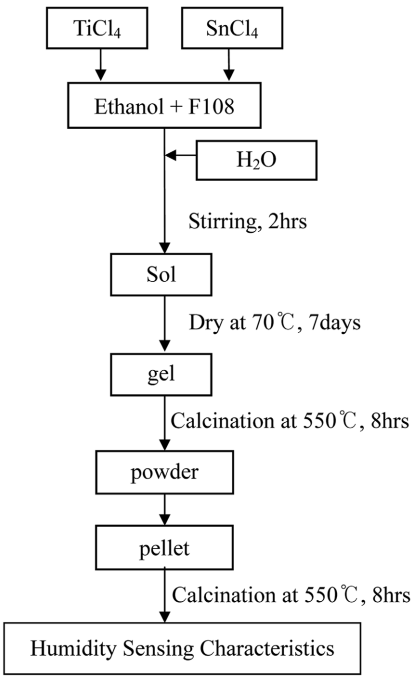


**Scheme 1**. Schemetic diagram of synthesis process for $TiO_2$-modified $SnO_2$.

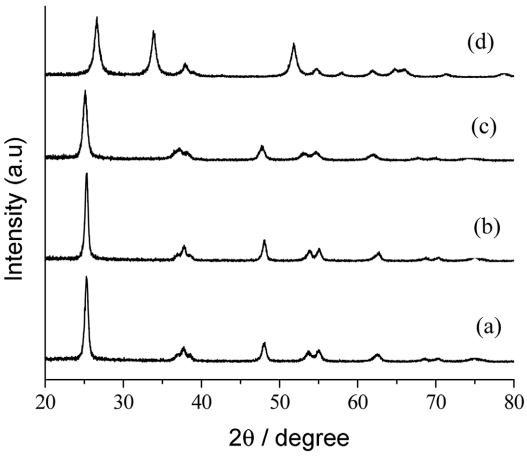


**Figure 1**. XRD patterns of (a) $TiO_2$, (b) $Ti_{0.9}Sn_{0.1}O_2$, (c) $Ti_{0.7}Sn_{0.3}O_2$ and (d) $SnO_2$.

1.0. $TiO_2$ crystallizes in anatase phase under present experimental conditions and the structure parameters are in agreement with reference data. (JCPDS file no. 21-1272). Structural parameters of $SnO_2$ also match with the reported data (JCPDS file no. 21-1250). For all other compositions, the product is multiphase, and XRD lines matche with those reported for $TiO_2$ and $SnO_2$ (not shown).

From the XRD study, the inference is that $SnO_2$ forms solid solution with $TiO_2$ in the composition range $0 < x < 0.3$ and crystallizes in anatase phase.

Apart from forming solid solution with $TiO_2$, addition of $SnO_2$ also affects the crystallite size and particle size of the composition. Figure 2 shows the SEM images of corresponding compositions studied by XRD. Table 1 summarizes the observations of structural and textural properties. An important observation is that the surface area increases and particle size decreases with increasing concentration of $SnO_2$.

Arresting particle growth by additives is a well established ceramic technique. In general, when the additive ions are not

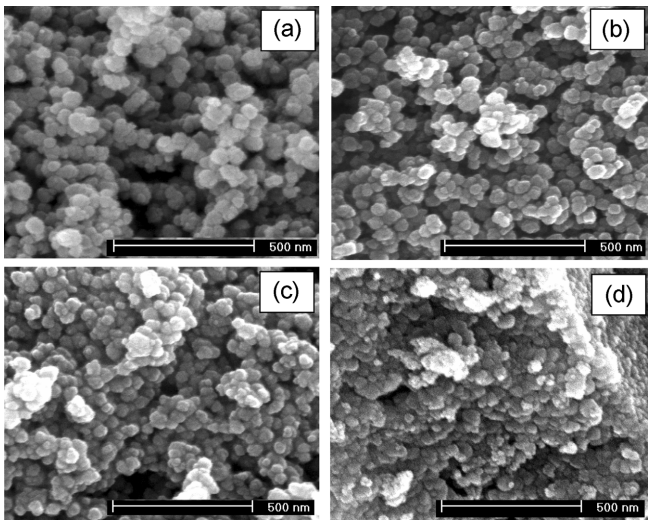


**Figure 2**. SEM image of (a) $TiO_2$, (b) $Ti_{0.9}Sn_{0.1}O_2$, (c) $Ti_{0.7}Sn_{0.3}O_2$ and (d) $SnO_2$.

**Table 1**. Structure and texture properties of $TiO_2$-modified $SnO_2$

| $Ti_{1-x}Sn_xO_2$ | Unit Cells | | | $S_{BET.}$ | Particle size | |
|---|---|---|---|---|---|---|
| | a (Å) | c (Å) | Vol. (Å) | ($m^2$/g) | SEM (nm) | XRD (nm)[a] |
| x = 0 | 3.7685 | 9.4690 | 134.4 | 46 | 62 | 23 |
| x = 0.1 | 3.7773 | 9.4974 | 135.5 | 47 | 46 | 19 |
| x = 0.3 | 3.7642 | 9.4590 | 134.0 | 54 | 39 | 14 |
| x = 1.0 | 4.7331 | 3.1842 | 61.3 | 28 | 43 | 21 |

[a]The crystallite size was calculated using Seherer equation from XRD.

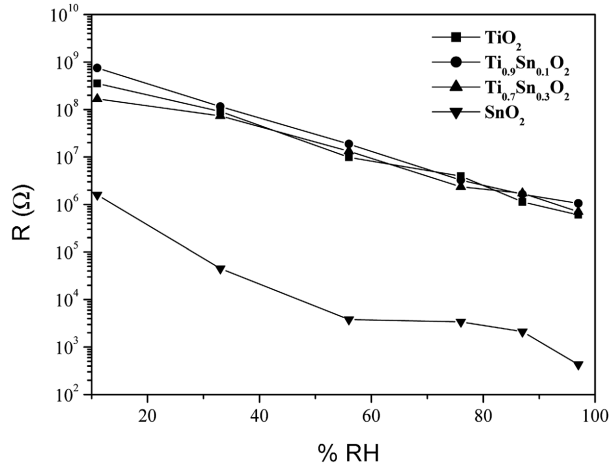


**Figure 3**. Dependency of the resistance of $TiO_2$-modified $SnO_2$ on relative humidity.

accommodated in the lattice, they tend to segregate at the grain boundaries of host particles. In the present case, $Sn^{4+}$ having much bigger size (83 pm) than $Ti^{4+}$ (74.5 pm) is expected to take lattice site. From XRD study, a trend is clearly shown that $Sn^{4+} > 0.3$ can not take $TiO_2$ lattice site as is expected. Therefore, it is reasonable to suggest that, at a low temperature of formation (500 °C), only a part of the $Sn^{4+}$ takes lattice site for all the compositions, while the remaining part gets segregated at the $TiO_2$ grain boundaries, thus arresting particle growth.

Figure 3 shows the humidity sensitivity of single phase compositions in terms of resistance variation as a function of relative humidity (RH) at a fixed ambient temperature of 25 °C. As the RH increases the resistance decreases by three orders in RH range 11 to 97%. The change is linear for the all composites except for pure $SnO_2$, suggesting that mechanism of resistance variation is similar over the region of 11-97%. However, in case of $SnO_2$ the resistance (R) vs RH plot is clearly nonlinear for the RH > 60%. The nonlinearity of $SnO_2$ sample might be due to the inhomogenous absorption of water molecule. For clarity, a representative humidity sensitivity curve for the composition $Ti_{0.9}Sn_{0.1}O_2$ is shown in Figure 4.

$TiO_2$ is known to be hydrophilic because of the dissociative adsorption of water at $Ti^{3+}$ defect sites on the surface of the particles.[15] Also, the mechanism of $TiO_2$ based humidity sensors is explained as the decrease in resistance of sensing

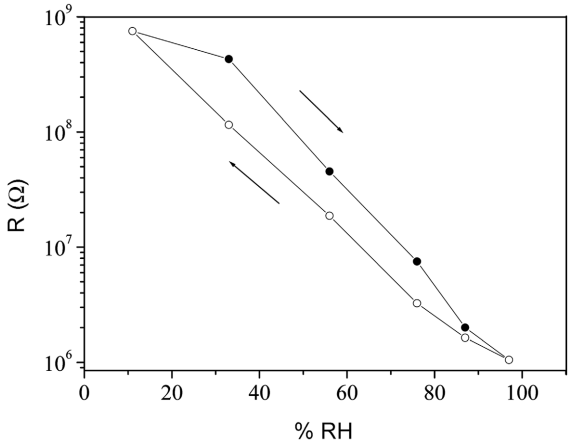


**Figure 4**. Absorption-desorption behavior of $Ti_{0.9}Sn_{0.1}O_2$ under different humidity conditions.

element because of proton conduction. These protons become available from adsorption of water. Thus, higher adsorption of water causes decrease in R with increasing RH. $Sn^{4+}$ doping decreases the particle size thus increasing the surface area. Also it may be mentioned that the particle size is in the nanometer range. This enhances the sensitivity of $TiO_2$ based material for RH.[16] Also, during synthesis, polymeric surfactant has been used which helped to form porous powder. This is observed by BET surface area measurements of one composition (see supplementary information). Such pores are reported to add electrolytic conduction contribution to protonic conduction enhancing the sensitivity.[17] It may be noted that the nonlinearity in sensitivity curve for $SnO_2$ is at high RH > 60%. This may occur due to condensation of water which disturbs equilibrium adsorption-desorption process.

Although the doping of $Sn^{4+}$ increases the surface area of powders, responsible for humidity sensitivity, the segregation of $Sn^{4+}$ at grain boundaries would be unfavorable factor as hydrophilicity of $TiO_2$ would decrease. This is reflected in the study of various compositions in our study. x = 0.1 gives better results with respect to sensitivity and minimum hysteresis than x = 0.2, 0.3, although these compositions are superior to the x = 0.1 composition in terms of lower particle size and hence higher surface area.

In summary, $Ti_{1-x}Sn_xO_2$ compositions in the range ($0 < x < 0.3$) form a solid solution by sol-gel method and show improved humidity sensing property when compared to pure $TiO_2$. The lowering of particle size by addition of $Sn^{4+}$ and the effect of F127 to achieve porous powder is proposed to be a cause of better humidity sensitivity.

## Experimental Section

The powders to make ceramic sensors were prepared by sol-gel process. $TiCl_4$ and $SnCl_4{\cdot}5H_2O$ were used as precursors for synthesizing $TiO_2$ and $SnO_2$ respectively. The precursor chlorides were purchased from Aldrich Chemicals and used without any further processing. A triblock polymer, $(HO(CH_2CH_2O)_{106}(CH_2CH(CH_3)O)_{70}(CH_2CH_2O)_{106}H)$ designated $EO_{106}PO_{70}EO_{106}$ was dissolved in 10 gm of ethanol (EtOH), 0.01 mole. Titanium precursor solution in EtOH was added to the continuously stirred surfactant solution. Vigorous stirring was continued for two hours at room temperature after addition of precursor. To avoid precipitation, chelating agent, namely, acetyl acetone was added in the required mole ratio to completely complex the metal species. The resulting sol was allowed to gel in an open Petri dish at 60 °C in air for 6 days. The gel thus obtained was then calcined at 550 °C for 8 hours to remove surfactant.

To study the effect of tin addition in $TiO_2$, a mixture of titanium tetrachloride and tin tetrachloride was processed so that finally $Ti_{1-x}Sn_xO_2$ would form where $0 < x < 1$.

Sensor characterization was done by measuring resistance of the pellets on Keithley multimeter. Applying silver paste on the two faces of the pallets and heating the sample at 300 °C, proper contacts were assured. D.C. resistance measurements were done in dark in a suitable cell where temperature and humidity were monitored. Alla portable digital thermohydrogram was employed to measure relative humidity with 1% accuracy. For high resistance samples, current response, at different voltages was studied as a function of relative humidity, varied in the steps of 20% in the range 11 to 97%. The nitrogen adsorption/desorption isotherms at 77 K were measured using a Micromeritics ASAP 2400 system to estimate surface areas, pore volumes, and pore size distribution, and and pore size distributions were calculated by the BJH method. Sensor materials were characterized by XRD, BET and SEM.

**Acknowledgements.** This work was supported by the Korea Ministry of Commerce, Industry and Energy (MOCIE) through the Research Center for Nanocatalysis and Institutional Research Program (KRICT) and Nano Center for Fine Chemicals Fusion Technology. S. D. Sathaye greatfully acknowledge the financial support by KOFST. Authors thank to Dr. I. S. Mulla and Mr. Niranjan for their useful discussion.

**Supplementary information** is available *via* the internet at *http://www.kcsnet.or.kr/bkcs*.

## References

1. Tai, W.-P.; Oh, J. H. *Sens. Actuators B* **2002**, *85*, 154.
2. (a) Tai, W.-P.; Kim, J. G.; Oh, J. H. *Sens. Actuators B* **2003**, *86*, 477. (b) Ganjali, M. R.; Zamani, H. A.; Norouzi, P.; Adib, M.; Rezapour, M.; Aceedy, M. *Bull. Korean Chem. Soc.* **2005**, *26*, 579.
3. (a) Huang, S.-J.; Lee, H.-K.; Kang, W.-H. *Bull. Korean Chem. Soc.* **2005**, *26*, 241. (b) Gusmano, G.; Montesperelli, G.; Nunziante, P.; Traversa, E.; Montenero, A. *J. Ceram. Soc. Jpn.* **1993**, *101*, 1095.
4. Jain, M. K.; Bhatnagar, M. C.; Sharma, G. L. *Sens. Acturators B* **1999**, *55*, 180.
5. Innocenzi, P.; Martucci, A.; Guglielmi, M.; Bearzotti, A.; Traversa, E. *Sens. Acturators B* **2001**, *76*, 299.
6. Wu, Q.; Lee, K. M.; Liu, C. C. *Sens. Acturators B* **1993**, *13*, 1.

7. Gusmano, G.; Montesperelli, G.; Traversa, E.; Mattogno, G. *J. Am. Ceram. Soc.* **1993**, *76*, 743.
8. Fukazawa, M.; Matuzaki, H.; Hara, K. *Sens. Acturators B* **1993**, *14*, 521.
9. Bearzotti, A.; Montesperelli, G.; Traversa, E. *Sens. Acturators B* **1994**, *18-19*, 525.
10. Tai, W.-P.; Kim, J.-G.; Oh, J.-H. *Sens. Actuators B* **2003**, *96*, 477.
11. Uchikawa, F.; Shimamoto, K. *J. Am. Ceram. Soc. Bull.* **1985**, *64*, 1137.
12. Sadaoka, Y.; Sakai, Y.; Mitsui, S. *Sens. Acturators* **1988**, *13*, 147.
13. Ichinose, N.; Tanaka, Y. *Sens. Mater.* **1988**, *1*, 77.
14. Kim, T. Y.; Lee, D. H.; Shim, Y. C.; Bu, J. U.; Kim, S. T. *Sens. Acturators B* **1992**, *9*, 221.
15. Montesperelli, G.; Pumo, A.; Traversa, E.; Gusmano, G.; Bearzotti, A.; Montenero, A.; Gnappi, G. *Sens. Acturators B* **1995**, *24-25*, 705.
16. (a) Ramgir, N. S.; Hwang, Y. K.; Jhung, S. H.; Mulla, I. S.; Chang, J.-S. *Sens. Actuator B*, in press. (b) Ramgir, N. S.; Hwang, Y. K.; Jhung, S. H.; Kim, H.-K.; Hwang, J.-S.; Mulla, I. S.; Chang, J.-S. *Appl. Surf. Sci.*, in press.
17. Kazuhito, R. W.; Akira, H.; Makoto, F.; Eiichi, C.; Atsushi, K.; Mitsuhide, K.; Shimohigoshi, M.; Watanabe, T. *Adv. Mater.* **1998**, *10*, 135.
18. Tai, W.-P.; Oh, J.-H. *Sens. Actuators B* **2002**, *85*, 154.